Available online at
https://jmeche.uitm.edu.my/

e-ISSN: 2550-164X

Journal of Mechanical Engineering 22(2) 2025, 97 – 110.

Journal of Mechanical Engineering

Impact of Body Weight on Intervertebral Disc: A Finite Element Analysis of Lumbar Spine Total Disc Replacement

Siti Nurfaezah Zahari[1], Mohd Juzaila Abd Latif[1,2*], Mohamad Shukri Zakaria[1,2], Masni Azian Akiah[3], Nguyen Ho Quang[4], Mohammed Rafiq Abdul Kadir[5]

[1]Fakulti Teknologi dan Kejuruteraan Mekanikal (FTKM), Universiti Teknikal Malaysia Melaka (UTeM), Hang Tuah Jaya, 76100 Durian Tunggal, Melaka, Malaysia.

[2]Centre for Advanced Research on Energy (CARe), Universiti Teknikal Malaysia Melaka (UTeM), Hang Tuah Jaya, 76100 Durian Tunggal, Melaka, Malaysia.

[3]Fakulti Teknologi dan Kejuruteraan Industri dan Pembuatan (FTKIP), Universiti Teknikal Malaysia Melaka (UTeM), Hang Tuah Jaya, 76100 Durian Tunggal, Melaka, Malaysia

[4]Institute of Engineering and Technology, Thu Dau Mot University, Thu Dau Mot City, Binh Duong Province, Vietnam.

[5]Department of Biomedical Engineering, Faculty of Engineering, Universiti Malaya 50603 Kuala Lumpur, Malaysia.

ARTICLE INFO

Article history:
Received 7 August 2024
Revised 5 November 2024
Accepted 29 December 2024
Online first
Published 15 May 2025

Keywords:
Lumbar spine
Total disc replacement
Intersegmental rotation
Nucleus pressure
Annulus stress

DOI:
https://doi.org/10.24191/jmeche.v22i2.6180

ABSTRACT

Total disc replacement is a frequently performed surgical intervention for managing severe degenerative disc disease, aiming to maintain lumbar spine mobility. Nevertheless, long-term outcomes have highlighted concerns such as spinal instability and degeneration of adjacent segments. This study explores the biomechanical implications of body weight on adjacent vertebral segments in a lumbar spine implanted with a total disc replacement prosthesis through finite element analysis. Detailed three-dimensional lumbar spine finite element models were developed, including both an intact spine and a spine with the Maverick prosthesis implanted at the L4-L5 segment, with verification against existing literature. The models underwent follower compression loads of 500 N, 800 N, and 1200 N, representing normal, overweight, and obese conditions, combined with pure moments of 7.5 Nm applied in flexion and extension. The analysis presented that increased body weight and the rigid characteristics of the Maverick prosthesis at the L4-L5 significantly influenced segmental motion, nucleus pulposus pressure, and annulus fibrosus stress compared to intact lumbar spine. The increasing body weight affected lumbar spine segmental motion, with the implanted lumbar spine model showing altered intersegmental rotation by 57% during extension motion. Additionally, notable increases in nucleus pulposus pressure and annulus fibrosus stress were observed, reaching 155% and 124% respectively, at the L3-L4 segment during extension under obese conditions. These biomechanical changes may contribute to early intervertebral disc damage and annular tear at the disc rim.

[1*] Corresponding author. *E-mail address*: juzaila@utem.edu.my
https://doi.org/10.24191/jmeche.v22i2.6180

INTRODUCTION

Low back pain (LBP), a pervasive musculoskeletal condition, often impacts quality of life by causing discomfort and disability. Increased body weight is a well-known contributor to joint stress, resulting in joint degeneration (Dario et al., 2015; Zhang et al., 2018). With the increasing prevalence of overweight and obesity, the occurrence of LBP is expected to escalate accordingly. Research has shown that excessive compressive loads on the spine lead to a reduction in the volume of the nucleus pulposus and a decrease in intervertebral disc (IVD) height (Nahorna & Baur, 2023; Segar et al., 2019). This degeneration subsequently damages the vertebral endplate and causes the outer annulus of the IVD to bulge, which is associated with pain initiation due to nervous system involvement (Bonnheim et al., 2022).

Total disc replacement (TDR) has emerged as a promising surgical solution for treating severe degenerative disc disease. Despite its potential, the long-term effectiveness of TDR remains uncertain. Uncontrolled long-term studies have observed that while TDR enhances mobility in the lumbar spine, it simultaneously increases pressure and stress on the IVD, potentially accelerating degeneration in adjacent segments (Lu et al., 2018; Park et al., 2016).

To date, most biomechanical data from in vitro and computational studies have explored the capability of prostheses to replicate the behaviour of intact discs and their long-term durability (Mazlan et al., 2017; Wen et al., 2024). Clinical studies on living subjects have reported that prosthetic devices such as Charité®, Prodisc®, and Maverick® restored disc height and range of motion (ROM) without disrupting sagittal balance (Liang et al., 2024). However, a five-year clinical study on patients with Charité® replacements noted modifications in lumbar curvature, increased translation, and ROM post-implantation at the L4-L5 segment (Lu et al., 2018). Additionally, a ten-year study of the AcroFlex® prosthesis found it inadequate in preventing disc degeneration at adjacent segments (Furunes et al., 2018). Conversely, an in vitro study of the Maverick® prosthesis on a cadaveric lumbar spine indicated that its rigidity was comparable to the intact state (Zigler et al., 2018).

Computational studies utilizing the finite element method have extensively investigated the biomechanical effects of lumbar prostheses. Prosthetic devices such as Charité®, Prodisc®, and Slide-disc® have been found to alter the motion of the lumbar spine at the implanted segment (Ke et al., 2024; Suarin et al., 2021). These biomechanical outcomes depend more on individual spinal anatomy than specific prosthesis designs. Achieving optimal restoration of lumbar spine biomechanics involves selecting the appropriate prosthesis height and position, preserving critical structures such as the anterior longitudinal ligament (ALL) and the lateral annular fibres (Mabrouk et al., 2022). This is particularly important to address the instability and further degeneration observed at both the operated and adjacent segments following TDR surgery. Furthermore, modifications in lumbar spine segmental motion increase facet joint force at both the operation and adjacent lumbar segments, potentially leading to facet degeneration (Suarin et al., 2021).

It is essential to understand the effects of TDR post-surgery on the lumbar spine particularly when subjected to excessive compressive loads. Moreover, the relationship between increased body weight and stress during various body movements needs further elucidation. Therefore, this study aims to examine the intersegmental rotation, nucleus pulposus pressure, and annulus fibrosus stress of Maverick® prosthesis implanted lumbar spine at adjacent vertebral segments using finite element analysis. The Maverick® prosthesis is extensively studied in clinical, and experimental research due to its role in spinal motion preservation and potential as an alternative to spinal fusion (Blumenthal & Ohnmeiss, 2024; Gornet et al., 2019). This research seeks to deepen the understanding of how TDR and obesity interact to influence the lumbar spine biomechanics.

https://doi.org/10.24191/jmeche.v22i2.6180

METHODOLOGY

Model Development and Segmentation

A three-dimensional lumbar spine finite element (FE) model was constructed using computed tomography (CT) scan data from a 21-year-old healthy male subject (173 cm in height and 70 kg in weight), with ethical approval secured (UTeM.47.01.01/500-25/16(13)). Vertebral segmentation was achieved through Mimics software, while the soft tissues of the IVD and facet joint cartilage were modelled using Mimics and SolidWorks 2022 software as shown in Fig 1. The facet joint cartilage, essential for regulating spinal movement, was modelled with a uniform thickness of 2 mm. An initial gap of 0.5 mm was incorporated between cartilage surfaces to reflect natural anatomical conditions.

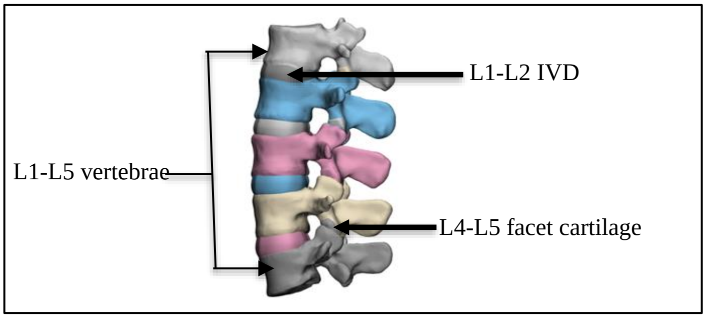

Fig. 1. Three-dimensional lumbar spine model.

Construction of Intervertebral Disc and Ligaments

The IVD and ligament construction was based on previous work (Zahari et al., 2017). The IVD was subdivided into annulus fibrosus and nucleus pulposus with a volumetric ratio of 3:7. The annulus fibrosus was further partitioned into four zones which were external ventral-lateral (EVL), internal ventral-lateral (IVL), external dorsal (ED), and internal dorsal (ID), as shown in Fig 2. This segmentation was necessary for constructing and defining the annulus fibres' orientation to reinforce the tissue with collagenous fibres.

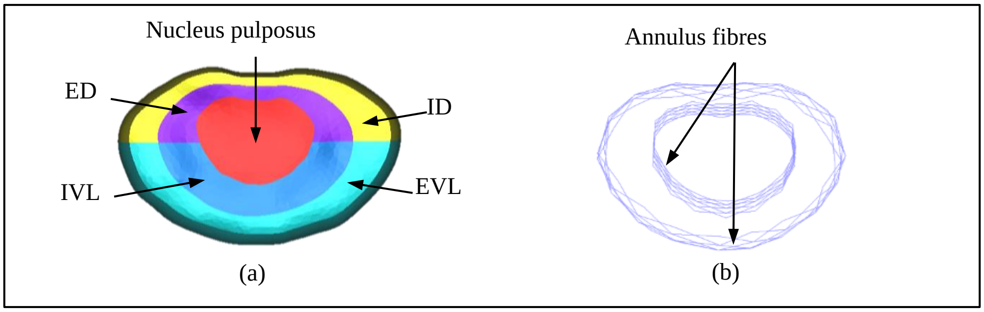

Fig. 2. Construction of IVD (a) regional classification of IVD (b) orientation of annulus fibres.

The annular fibres with radial alignment, ranging from ±24º on the ventral side to ±46º on the dorsal side, replicating natural fibre orientation observed in anatomical studies. The fibres were represented as three-dimensional two-node truss elements, connecting inner and outer annular regions as well as the nucleus and inner annulus, as shown in Fig 2(b). Meanwhile, three-dimensional truss elements were used

https://doi.org/10.24191/jmeche.v22i2.6180

to model ligaments under tension conditions, with cross-sectional areas based on previous studies as shown in Table 1.

Table 1. Cross-sectional area of ligaments (Zahari et al., 2017)

Ligament	Cross-sectional area (mm^2)
Posterior longitudinal ligament (PLL)	20.0
Anterior longitudinal ligament (ALL)	63.7
Ligamentum flavum (LF)	40.0
Capsular ligament (CL)	30.0
Intertransverse ligament (ITL)	1.8
Interspinous ligament (ISL)	40.0
Supraspinous ligament (SSL)	30.0

Finite Element Model of Lumbar Spine

The FE models, representing both an intact lumbar spine and one implanted with a Maverick® prosthesis, were developed using Marc/Mentat finite element software. The Maverick® prosthesis was modelled according to specified dimensions, using linear elastic material characterized by an elastic modulus of 300 GPa, Poisson's ratio of 0.27, and friction coefficient of 0.05 (Gstoettner et al., 2008). For prosthesis implantation at the L4-L5 segment, the nucleus and ALL were completely removed. Partial preservation of the lateral annulus was maintained according to the size of the endplates. Anterior placement of the implant was achieved through an idealized surgical approach, assuming perfect osteointegration between the prosthesis and the bone. The nucleus at the central IVD space served as the reference point for prosthesis positioning. Fig 3 shows both the intact and implanted osseoligamentous lumbar spine FE models.

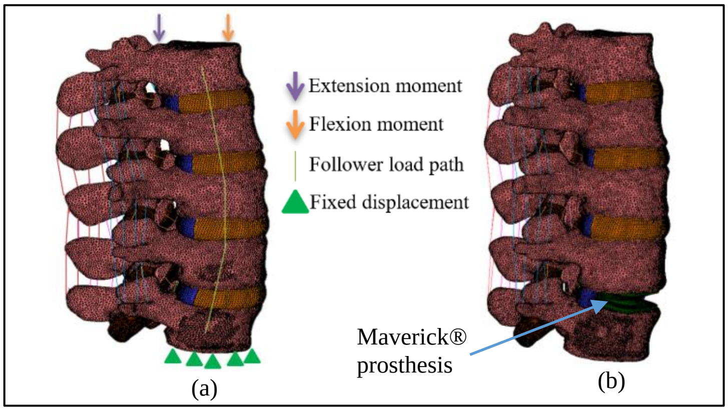

Fig. 3. FE model of lumbar spine (a) intact (b) implanted.

Material Properties and Contact Interactions

Material properties for all model components are summarized in Table 2. Cortical and cancellous bones were modelled as linear isotropic materials, while the nucleus and annulus were represented by Mooney-Rivlin hyperelastic model. The stress-strain behavior of the annulus fibres and ligaments was based on non-linear relationships consistent with physiological responses under tension (Zahari et al., 2017).

The IVD and vertebral interfaces were modelled as perfectly bonded to ensure stability and facilitate load transfer during simulation. Contact between the facet joint cartilage surfaces was treated as surface-to-surface interaction with a normal contact stiffness of 200 N/mm and zero friction coefficient to simulate

https://doi.org/10.24191/jmeche.v22i2.6180

the lubricating effects of synovial fluid for frictionless motion (Zahari et al., 2017). An initial gap of 0.5 mm was maintained between opposing cartilage surfaces to replicate natural joint spacing.

Table 2. Material properties of lumbar spine FE model (Zahari et al., 2017)

Element set	Element type	Material properties
Vertebrae bone		
Cortical bone	3-D Tetrahedron	E = 12000 MPa, ν = 0.3
Cancellous bone	3-D Tetrahedron	E = 100 MPa, ν = 0.2
Articular cartilage	3-D Herman formulation, lower order tetrahedron	E = 35 MPa, ν = 0.4
Intervertebral disc		
Nucleus pulposus	3-D Herman formulation, lower order tetrahedron	Mooney Rivlin: $C_1 = 0.12$, $C_2 = 0.03$
Annulus ground substance	3-D Herman formulation, lower order tetrahedron	Mooney Rivlin: $C_1 = 0.18$, $C_2 = 0.045$
Ligaments		
Posterior longitudinal	3-D Truss	E = 10.0 MPa (ε<11%), E = 20 MPa (ε >11%)
Anterior longitudinal	3-D Truss	E = 7.8 MPa (ε <12%), E = 20 MPa (ε >12%)
Ligamentum flavum	3-D Truss	E = 15.0 MPa (ε <6.2%), E = 19.5 MPa (ε >6.2%)
Capsular ligament	3-D Truss	E = 7.5 MPa (ε <25%), E = 32.9 MPa (ε >25%)
Intertransverse	3-D Truss	E = 10.0 MPa (ε <18%), E = 58.7 MPa (ε >18%)
Interspinous	3-D Truss	E = 10.0 MPa (ε <14%), E = 11.6 MPa (ε >14%)
Supraspinous	3-D Truss	E = 8.0 MPa (ε <20%), E = 15.0 MPa (ε >20%)

Loading and Boundary Conditions

The FE models of both intact and prosthesis-implanted lumbar spines were subjected to combined loading conditions, including pure moments of 7.5 Nm and compressive follower loads, to simulate flexion and extension physiological activities. Moments were applied as force couples at the anterior and posterior regions of the L1 vertebral body as tabulated in Table 3. Concurrently, follower compressive loads representing upper body weight were distributed along the lumbar curvature using eight spring elements connected to the lateral regions of the L1-L5 vertebral bodies (Zahari et al., 2017). This approach stabilized the spine, emulated local muscular support, and prevented unnecessary moment generation, enabling higher load simulations.

Table 3. Force couple applied on the lumbar spine FE model (Zahari et al., 2017)

Loading direction	Anterior point		Posterior point	
	F_y (N)	F_z (N)	F_y (N)	F_z (N)
Flexion	-98	-230	98	230
Extension	98	230	-98	-230

The compressive loads of upper body weight, representing 60% - 70% of total body weight (including trunk, head, and arms), corresponded to body weights of 55 kg, 80 kg, and 150 kg to represent normal weight, overweight, and obese conditions, respectively (Kurutz & Oroszváry, 2010; Walpole et al., 2012). The follower loads were calculated as 300 N, 600 N, and 1000 N, with an additional 200 N included to account for muscular forces during flexion and extension. Meanwhile, the L5 vertebra's inferior surface was constrained in all directions to simulate fixed boundary conditions.

https://doi.org/10.24191/jmeche.v22i2.6180

RESULTS AND DISCUSSION

Verification of FE Model

The FE model representing the L1-L5 osseoligamentous lumbar spine was initially verified by comparing its range of motion (ROM) under a pure moment of 7.5 Nm during flexion and extension with published in vitro data (Panjabi et al., 1994). The intersegmental rotation of the FE model exhibited a pattern consistent with the experimental results, as depicted in Fig 4. The deviation in ROM during flexion was measured at 7.5% under the 7.5 Nm moment. While noticeable discrepancies were present between 2 Nm and 5 Nm during extension, the ROM deviation reduced to 8.1% at 7.5 Nm. The FE model demonstrates a high degree of accuracy in replicating physiological lumbar spine motion observed in in vitro studies, with less than a 15% acceptable threshold given the complexity of human tissue behavior and variability in biological responses (Xu et al., 2017).

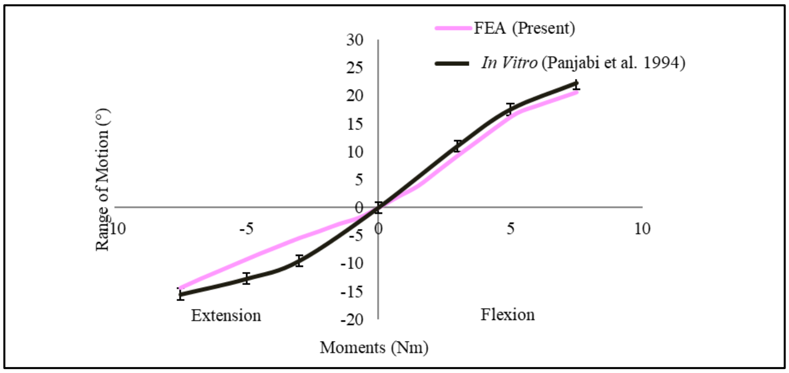

Fig. 4. Comparison of total ROM between the present FE model and previous in vitro study.

Further verification was performed by assessing the axial displacement and intradiscal pressure of the L4-L5 IVD segment. Fig 5 illustrates that these results were well aligned with previous in vitro findings (Ranu, 1990). Under a compression load of 1200 N, the axial displacement and intradiscal pressure deviated by 7.1% and 6.9%, respectively, compared to the previous in vitro study.

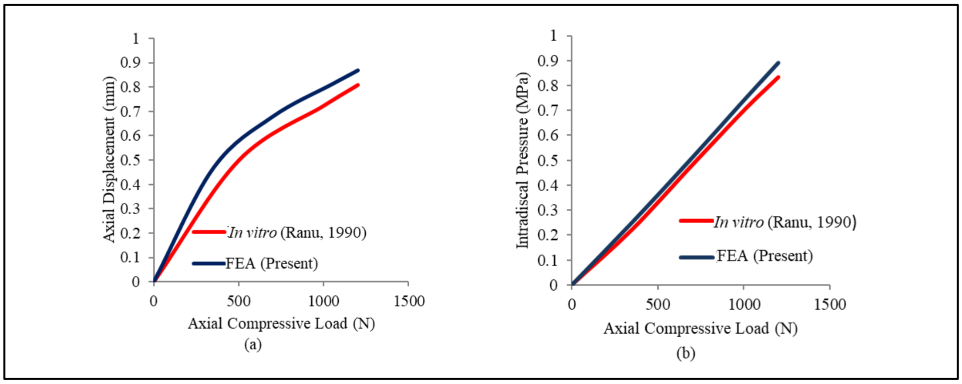

Fig. 5. Axial displacement and intradiscal pressure under compressive load.

https://doi.org/10.24191/jmeche.v22i2.6180

Subsequently, the intersegmental rotations of the implanted FE model subjected to normal compressive load at L1-L2 and L3-L4 lumbar segments were found to be within the range measured in previous in vitro biomechanics study of TDR using Maverick prosthesis as shown in Fig 6 (Wido et al., 2009). Although the intersegmental rotation at the L2-L3 lumbar segment was slightly higher, with a 33% difference, rotations across other segments showed variations of less than 4%, confirming reasonable agreement with experimental findings.

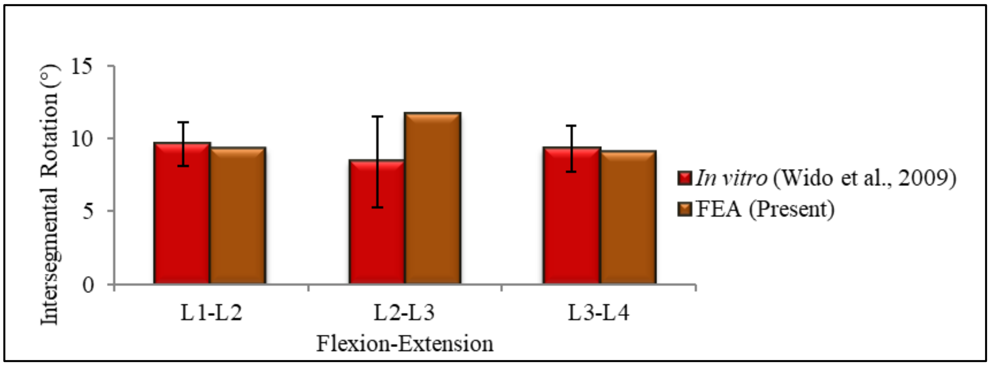

Fig. 6. Intersegmental rotation during flexion-extension between the present and previous in vitro study for the implanted lumbar spine model.

With both intact and implanted FE models verified, the study proceeded to evaluate the biomechanical behaviour of varying human weights (normal, overweight, and obese conditions) on the segmental motion and the IVD stresses in the lumbar spine. Changes in IVD stresses were assessed by measuring the intradiscal pressure and annulus fibrosus stress.

Intersegmental Rotation

The implanted lumbar spine FE model was subjected to varied loading conditions to explore their influence on intersegmental rotation. Fig 7 illustrates that human weight significantly affected segmental motion, with rotations increasing during spinal flexion and decreasing during. The most notable differences were observed at the L3-L4 segment. During extension, rotations increased by 6% and 10% for overweight and obese conditions, respectively, whereas in flexion, these differences were 1.8% and 5.4%. For other lumbar segments, the differences in intersegmental rotations of overweight and obese compared to normal conditions in extension were 1.8% - 2.3% and 3.5% - 4.5%, respectively, and in flexion, these differences were 1.7% - 2.1% and 3.5% - 4.2%, respectively.

Comparing the intact and implanted models showed an increase in intersegmental rotation at adjacent segments in both flexion and extension across all weight conditions as illustrated in Fig 8. However, the TDR was more significant in extension motion, particularly at the L3-L4 segment under obese conditions, which showed a 57% difference compared to the intact model. During flexion, the percentage differences in intersegmental rotation across all loading conditions ranged from 2% to 12%.

Similar FE studies have reported that under normal compressive load, the rotation at adjacent segments increased to 24% compared to the intact model (Smajic et al., 2022). Experimental studies further corroborated these observations, with Maverick prosthesis showing increases in intersegmental rotation for both flexion and extension (Wido et al., 2009). Previous study was also reported a 50% increase in ROM during flexion and a 30% increase during extension with the Maverick prosthesis (Bonnheim et al., 2021). These findings suggest that increased body weight combined with the rigidity of the prosthesis amplifies

https://doi.org/10.24191/jmeche.v22i2.6180

segmental motion at adjacent levels, potentially accelerating mechanical alterations in the lumbar spine post-implantation.

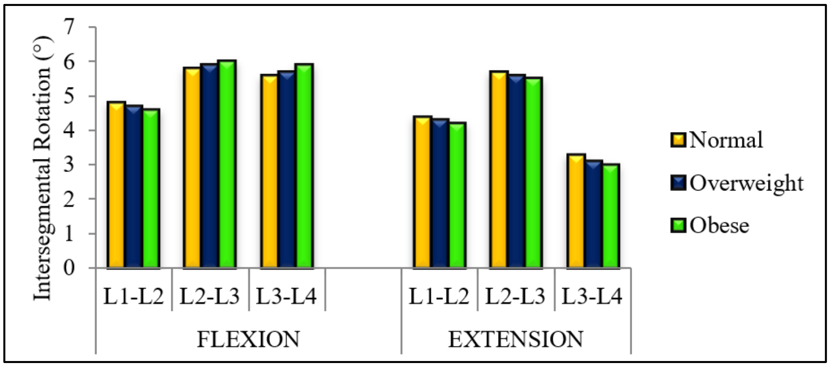

Fig. 7. Intersegmental rotation during flexion and extension under varying weight conditions.

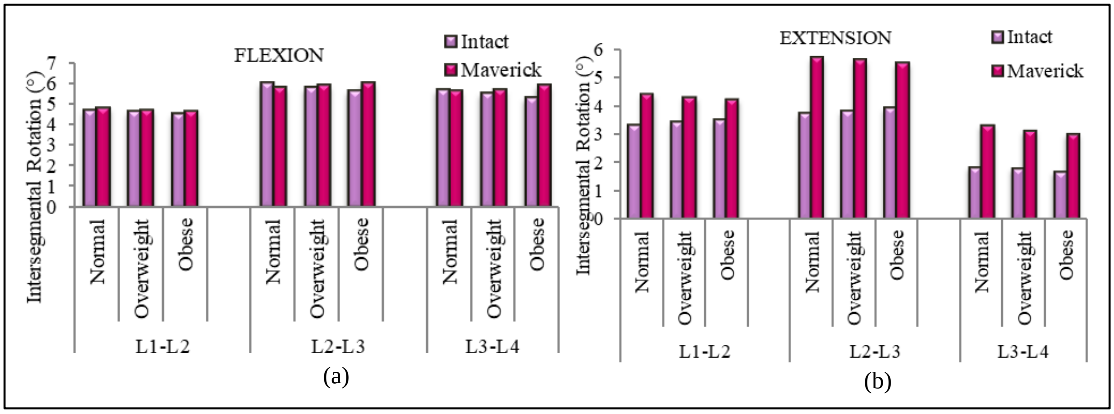

Fig. 8. Intersegmental rotation at adjacent segments of intact and implanted models in (a) flexion (b) extension.

Nucleus Intradiscal Pressure

Intradiscal pressure in the nucleus pulposus during flexion was generally higher than during extension across all loading conditions. As shown in Fig 9, the L2-L3 segment recorded the highest intradiscal pressure at 1.23 MPa during flexion under normal loading, while the lowest pressure of 0.17 MPa was observed during extension under obese conditions. Notable variations in intradiscal pressure were found at the L3-L4 segment in both flexion and extension motions. In flexion, overweight and obese conditions increased pressure by 4% and 11% respectively, compared to normal weight. During extension, these differences were more significant, reaching 10% and 20%, respectively. For other segments, the differences in intradiscal pressures between the normal and overweight conditions were 2.4% - 2.6% in flexion and 4.8% - 6% in extension. For obese conditions, these differences were 4.95% - 5.3% in flexion and 11% - 12% in extension.

Comparisons between intact and implanted lumbar spine models highlighted significant differences in nucleus pressure, particularly at the L3-L4 segment during extension as shown in Fig 10. After TDR, the nucleus pressure at this segment under obese load conditions increased tenfold compared to normal load

https://doi.org/10.24191/jmeche.v22i2.6180

conditions. These findings align with a previous study, which reported elevated nucleus pressure at adjacent segments in both flexion and extension following TDR (Wang et al., 2013). The results suggest that segments treated with artificial discs transfer substantial nucleus pressure to adjacent segments.

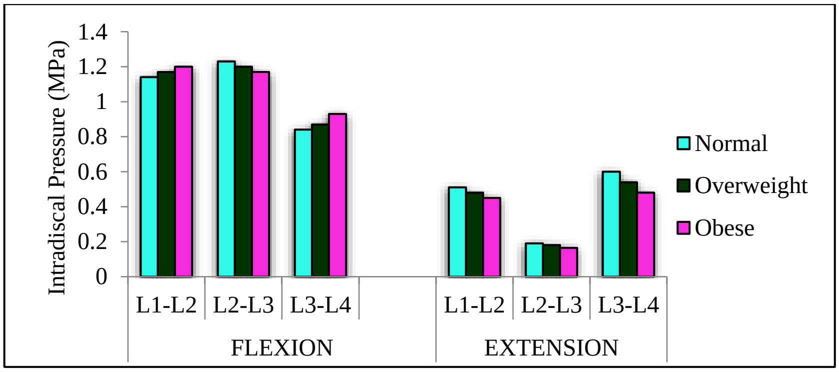

Fig. 9. Intradiscal pressure at adjacent segments for implanted lumbar spine under various loading conditions.

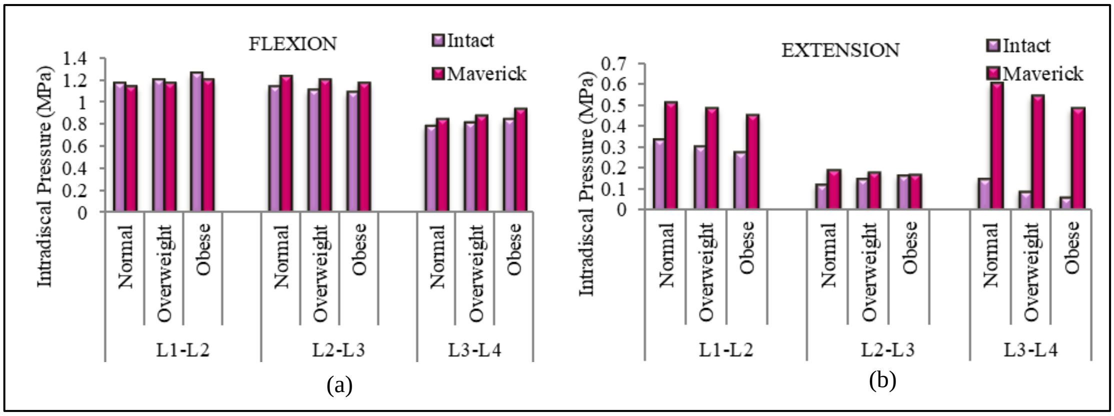

Fig. 10. Intradiscal pressure between the intact and implanted lumbar spine under various loading conditions during (a) flexion (b) extension.

Annulus Fibrosus Stress

The annulus stresses in extension motion were consistently higher than in flexion motion across all loading conditions as illustrated in Fig 11. The highest annulus stress of 6.1 MPa was observed at the L3-L4 segment under obese condition during extension. Conversely, the lowest annulus stress with 1.4 MPa was recorded at the L3-L4 segment during flexion.

The comparison between intact and implanted lumbar spine models showed significant increases in annulus stress at adjacent segments in both flexion and extension, particularly at the L3-L4 lumbar segment. Fig 12 illustrates that extension under obese load conditions resulted in a 124% increase in annulus stress compared to the intact lumbar spine, while flexion led to a 23% increase.

Stress contours shown in Fig 13 indicate that excessive stress at the operated level is transferred to adjacent lumbar segments, particularly the posterior IVD during spinal extension. This phenomenon could lead to a high potential for disc degeneration at adjacent lumbar segments after TDR surgery (Kitzen et al.,

https://doi.org/10.24191/jmeche.v22i2.6180

2021), which then potentially lead to structural failures such as annulus tears at the disc rim and herniation of the disc (Korhonen et al., 2022).

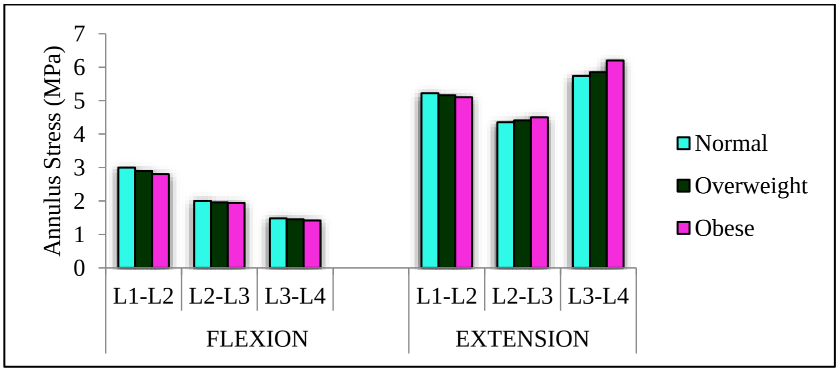

Fig. 11. Annulus stress at adjacent segments of the implanted lumbar spine under various loading conditions.

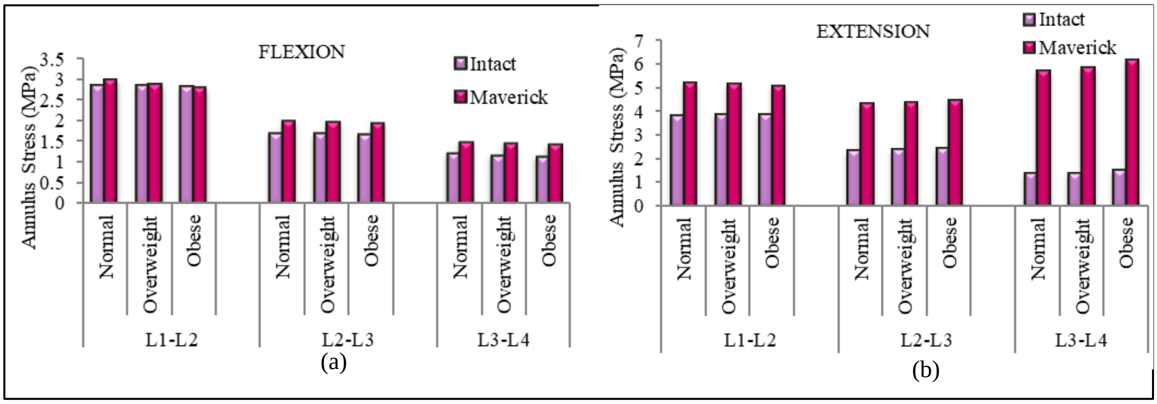

Fig. 12. Annulus stress between intact and implanted lumbar spine under various loading conditions during (a) flexion (b) extension.

https://doi.org/10.24191/jmeche.v22i2.6180

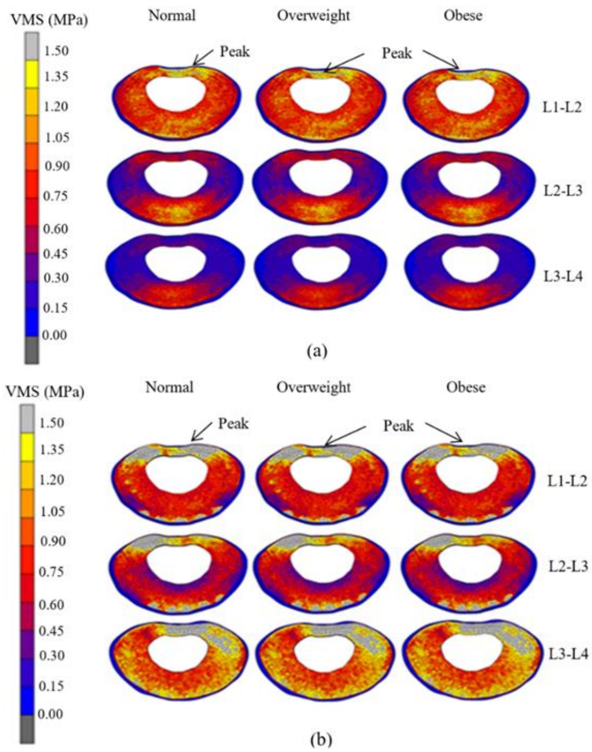

Fig. 13. Stress contours in annulus ground of annulus fibrosus at adjacent segments for the implanted lumbar spine during (a) flexion (b) extension.

CONCLUSION

The present study utilized FE models to examine the biomechanical impact of body weight on segmental motion, nucleus pressure, and annulus stress in both intact and implanted lumbar spines. The findings indicate that increasing body weight significantly elevates IVD stresses, with notable increases in nucleus pulposus pressure and annulus fibrosus stress. Flexion and extension motions impact these structures differently, where flexion increases the nucleus pulposus pressure while extension increases the stress on the annulus fibrosus. Heavier individuals are thus expected to experience elevated lumbar spine stresses, irrespective of the spine's position. Consequently, increased body weight can lead to higher nucleus pressure and annulus fibrosus stress, potentially contributing to early IVD damage, particularly at the disc rim. This issue is further compounded in the lumbar spine implanted with Maverick prosthesis. The rigidity of the prosthesis at the operated segment significantly alters lumbar spine movement and increases IVD stresses, accelerating degeneration at adjacent segments.

ACKNOWLEDGEMENTS/FUNDING

The authors would like to acknowledge the financial support from the Ministry of Higher Education Malaysia (ERGS/2012/FKM/TK01/02/3/E00005) and other support from Universiti Teknikal Malaysia Melaka (UTeM).

https://doi.org/10.24191/jmeche.v22i2.6180

CONFLICT OF INTEREST STATEMENT

The authors agree that this research was conducted in the absence of any self-benefits, commercial or financial conflicts and declare the absence of conflicting interests with the funders.

AUTHORS' CONTRIBUTIONS

The authors confirm their contribution to the paper as follows: **study conception and design**: Siti Nurfaezah Zahari, Mohd Juzaila Abd Latif; **funding acquisition**: Mohd Juzaila Abd Latif; **software**: Mohammed Rafiq Abdul Kadir; **methodology**: Mohd Juzaila Abd Latif, Mohamad Shukri Zakaria; **data collection**: Siti Nurfaezah Zahari; **analysis and interpretation of results**: Siti Nurfaezah Zahari, Mohd Juzaila Abd Latif, Mohammed Rafiq Abdul Kadir; **draft manuscript preparation**: Siti Nurfaezah Zahari, Masni Azian Akiah, Nguyen Ho Quang. All authors reviewed the results and approved the final version of the manuscript.

REFERENCES

Blumenthal, S. L., & Ohnmeiss, D. D. (2024). The scientific evidence for lumbar total disk replacement surgery. Indian Spine Journal, 7(2), 142-147.

Bonnheim, N. B., Adams, M. F., Wu, T., & Keaveny, T. M. (2021). The role of vertebral porosity and implant loading mode on bone-tissue stress in the human vertebral body following lumbar total disc arthroplasty. Spine, 46(19), E1022–E1030.

Bonnheim, N. B., Wang, L., Lazar, A. A., Zhou, J., Chachad, R., Sollmann, N., Guo, X., Iriondo, C., O'Neill, C., Lotz, J. C., Link, T. M., Krug, R., & Fields, A. J. (2022). The contributions of cartilage endplate composition and vertebral bone marrow fat to intervertebral disc degeneration in patients with chronic low back pain. European Spine Journal, 31(7), 1866–1872.

Dario, A. B., Ferreira, M. L., Refshauge, K. M., Lima, T. S., Ordoñana, J. R., & Ferreira, P. H. (2015). The relationship between obesity, low back pain, and lumbar disc degeneration when genetics and the environment are considered: A systematic review of twin studies. Spine Journal, 15(5), 1106–1117.

Furunes, H., Hellum, C., Espeland, A., Brox, J. I., Småstuen, M. C., Berg, L., & Storheim, K. (2018). Adjacent disc degeneration after lumbar total disc replacement or nonoperative treatment: A randomized study with 8-year follow-up. Spine, 43(24), 1695–1703.

Gornet, M. F., Burkus, J. K., Dryer, R. F., Peloza, J. H., Schranck, F. W., & Copay, A. G. (2019). Lumbar disc arthroplasty versus anterior lumbar interbody fusion: 5-year outcomes for patients in the Maverick disc investigational device exemption study. Journal of Neurosurgery: Spine, 31(3), 347–356.

Ke, H., Guo, Y., Zhang, X., Yin, L., Nie, W., Zhao, Y., Zhao, B., Zhang, K., Wen, Y., Ji, B., & Zhang, M. (2024). Structural modification and biomechanical analysis of lumbar disc prosthesis: A finite element study. Clinical Biomechanics, 116, 106266.

Kitzen, J., Vercoulen, T. F. G., Schotanus, M. G. M., van Kuijk, S. M. J., Kort, N. P., van Rhijn, L. W., & Willems, P. C. P. H. (2021). Long-term residual-mobility and adjacent segment disease after total lumbar disc replacement. Global Spine Journal, 11(7), 1032–1039.

Korhonen, T., Pesälä, J., Järvinen, J., Haapea, M., & Niinimäki, J. (2022). Correlation between the degree

https://doi.org/10.24191/jmeche.v22i2.6180

of pain relief following discoblock and short-term surgical disability outcome among patients with suspected discogenic low back pain. Scandinavian Journal of Pain, 22(3), 526–532.

Kurutz, M., & Oroszváry, L. (2010). Finite element analysis of weightbath hydrotraction treatment of degenerated lumbar spine segments in elastic phase. Journal of Biomechanics, 43(3), 433–441.

Liang, Y., Qian, Y., Xia, W., Guo, C., Zhu, Z., Liu, H., & Xu, S. (2024). Adjacent segment degeneration after single- and double-level cervical total disc replacement: a cohort with an over 12-year follow-up. European Spine Journal, 33(1), 232–242.

Lu, S., Sun, S., Kong, C., Sun, W., Hu, H., Wang, Q., & Hai, Y. (2018). Long-term clinical results following Charite III lumbar total disc replacement. Spine Journal, 18(6), 917–925.

Mabrouk, M. S., Marzouk, S. Y., & Afify, H. M. (2022). A biomechanical analysis of prosthesis disc in lumbar spinal segment using three-dimensional finite element modelling. International Journal of Biomedical Engineering and Technology, 39(1), 1–21.

Mazlan, M. H., Todo, M., Yonezawa, I., & Takano, H. (2017). Biomechanical alteration of stress and strain distribution associated with vertebral fracture. Journal of Mechanical Engineering, 2(2), 123–133.

Gstoettner, M., Heider, D., Liebensteiner, M., & Bach, C. M. (2008). Footprint mismatch in lumbar total disc arthroplasty. European Spine Journal, 17(11), 1470–1475.

Nahorna, A., & Baur, H. (2023). Biomechanical and functional effects of abdominal obesity on activities of daily living in individuals with low back pain. Journal of Physical Education and Sport, 23(9), 2426–2434.

Panjabi, M. M., Oxland, T. R., Yamamoto, I., & Crisco, J. J. (1994). Mechanical behavior of the human lumbar and lumbosacral spine as shown by three-dimensional load-displacement curves. Journal of Bone and Joint Surgery, 76(3), 413–424.

Park, S. J., Lee, C. S., Chung, S. S., Lee, K. H., Kim, W. S., & Lee, J. Y. (2016). Long-term outcomes following lumbar total disc replacement using ProDisc-II: average 10-year follow-up at a single institute. Spine, 41(11), 971–977.

Ranu, H. S. (1990). Measurement of pressures in the nucleus and within the annulus of the human spinal disc: Due to extreme loading. Proceedings of the Institution of Mechanical Engineers, Part H: Journal of Engineering in Medicine, 204(3), 141–146.

Segar, A. H., Fairbank, J. C. T., & Urban, J. (2019). Leptin and the intervertebral disc: a biochemical link exists between obesity, intervertebral disc degeneration and low back pain—an in vitro study in a bovine model. European Spine Journal, 28(2), 214–223.

Smajic, S., Vujadinovic, A., Kasapovic, A., Aldakheel, D. A., Charles, Y. P., Walter, A., Steib, J. P., Maffulli, N., Migliorini, F., & Baroncini, A. (2022). The influence of total disc arthroplasty with Mobidisc prosthesis on lumbar spine and pelvic parameters: a prospective in vivo biomechanical study with a minimum 3 year of follow-up. Journal of Orthopaedic Surgery and Research, 17(1), 456.

Suarin, M. A., Latif, M. J. A., Zakaria, M. S., Harun, M. N., & Nguyen, H. Q. (2021). Effects of total disc replacement on range of motion and facet stress in lumbar spine using a finite element analysis. International Journal of Nanoelectronics and Materials, 14, 263–274.

Walpole, S. C., Prieto-Merino, D., Edwards, P., Cleland, J., Stevens, G., & Roberts, I. (2012). The weight of nations: An estimation of adult human biomass. BMC Public Health, 12, 439.

https://doi.org/10.24191/jmeche.v22i2.6180

Wang, W., Zhang, H., Sadeghipour, K., & Baran, G. (2013). Effect of posterolateral disc replacement on kinematics and stress distribution in the lumbar spine: a finite element study. Medical Engineering and Physics, 35(3), 357–364.

Wen, D. J., Tavakoli, J., & Tipper, J. L. (2024). Lumbar total disc replacements for degenerative disc disease: A systematic review of outcomes with a minimum of 5 years follow-up. Global Spine Journal, 14(6), 1827-1837.

Wido, D. M., Kelly, B. P., Foley, K. T., Morrow, B., Wong, P., Kiehm, K., Sin, A., Bertagnoli, R., & DiAngelo, D. J. (2009). Biomechanical comparison of lumbar disc prostheses: ProDisc-l, Charité, and Maverick disc implant systems. 25th Southern Biomedical Engineering Conference (pp. 223–226). Springer Berlin Heidelberg.

Xu, M., Yang, J., Lieberman, I. H., & Haddas, R. (2017). Lumbar spine finite element model for healthy subjects: development and validation. Computer Methods in Biomechanics and Biomedical Engineering, 20(1), 1–15.

Zahari, S. N., Latif, M. J. A., Rahim, N. R. A., Kadir, M. R. A., & Kamarul, T. (2017). The effects of physiological biomechanical loading on intradiscal pressure and annulus stress in lumbar spine: a finite element analysis. Journal of Healthcare Engineering, SI 1, 9618940.

Zhang, T. T., Liu, Z., Liu, Y. L., Zhao, J. J., Liu, D. W., & Tian, Q. B. (2018). Obesity as a risk factor for low back pain: a meta-analysis. Clinical Spine Surgery, 31(1), 22-27.

Zigler, J. E., Blumenthal, S. L., Guyer, R. D., Ohnmeiss, D. D., & Patel, L. (2018). Progression of adjacent-level degeneration after lumbar total disc replacement. Spine, 43(20), 1395–1400.

https://doi.org/10.24191/jmeche.v22i2.6180